CLLMM RESEARCH CENTRE | GOYDER INSTITUTE FOR WATER RESEARCH

Climate impacts on biogeochemistry, microbial ecology, and methane emissions in the CLLMM region

March 2026

Christopher Keneally, James Hensel, Qinqin You, Luke Mosley and Justin Brookes

The CLLMM Research Centre has the objective of developing and delivering locally driven, innovative, and impactful research that reflects community and First Nations priorities to provide an evidence base to address critical needs of the CLLMM region. The CLLMM Research Centre will also bring together our First Nations, local community and scientists to create and share knowledge, and support our well-informed and engaged community and empower our future generations to be part of the solution.

The Goyder Institute for Water Research Coorong, Lower Lakes and Murray Mouth (CLLMM) Research Centre, based in Goolwa SA, was established in 2023 through funding by the Australian Government.

Australian Government

Department of Climate Change, Energy, the Environment and Water

The Goyder Institute for Water Research is a partnership between the South Australian Government through the Department for Environment and Water CSIRO, Flinders University and Adelaide University.

Government of South Australia
Department for Environment and Water

CSIRO

Flinders University

Adelaide University

Title page photo credit: Methane chambers deployed at Parnka Point, facing the South Lagoon (Ms Qinqin You).

Enquires should be addressed to: CLLMM Research Centre
Level 1, 92 Barrage Road
Goolwa, SA 5214
e-mail: info@cllmmresearchcentre.org

This report may be cited as:

Keneally C, Hensel J, You Q, Mosley L, and Brookes J (2026). *Climate impacts on biogeochemistry, microbial ecology, and methane emissions in the CLLMM region*. A report prepared by Adelaide University for the Goyder Institute for Water Research CLLMM Research Centre, Goolwa. https://doi.org/10.25909/33159548.

Disclaimer

Table of Contents

Executive Summary

This report provides the first regional assessment of aquatic methane (CH_4) emissions across the Coorong, Lower Lakes, and Murray Mouth (CLLMM) region. It combines direct emissions measurement of CH_4 (a greenhouse gas with ~80× the warming effect of CO_2) with microbial community analysis, and habitat-informed climate-scenario estimates, to examine how CH_4 varies across freshwater, brackish, saline, and hypersaline environments in one of Australia's most important and climate-exposed wetland systems.

The report found that CH_4 emissions across the CLLMM could not be explained by the typical assumption that increasing salinity suppresses CH_4. Ebullition (bubble-mediated emissions) was confined to low-salinity waters, but diffusive emissions persisted across the entire salinity gradient, including in hypersaline habitat. Hydrological and organic-matter-related variables (including tide height, dissolved organic matter, sediment organic matter, dissolved oxygen, and barrage flows) were each more informative controls on emissions than salinity alone. These findings indicate that CH_4 emissions reflect interacting effects of organic-matter availability, oxygen conditions, hydrological connectivity, water residence time, and physical transport.

Methane-cycling microbial communities also changed systematically across the CLLMM's salinity gradient. Aerobic methane oxidisers (CH_4-consumers) were relatively enriched in fresher and moderately saline habitats, whereas methylotrophic methanogens (CH_4-producers) were more strongly associated with saline and hypersaline habitat. This suggests that salinity-related habitat change may alter the balance between methane production and consumption, potentially allowing diffusive emissions to persist even where CH_4 bubbles are suppressed.

Habitat-informed climate-scenario estimates suggest that Coorong lagoon CH_4 emissions may increase under hotter, drier future conditions, while greater marine influence and sea-level rise may produce only small reductions in emissions. Salinisation should therefore not be considered a reliable CH_4-mitigation pathway, particularly given its substantial ecological costs.

The results also show that hydrological interventions may produce both benefits and trade-offs for methane-cycling. Freshening, flushing, and improved oxygenation may reduce CH_4 accumulation and support oxidation, whereas inflows rich in nutrients or labile organic carbon may stimulate CH_4 production where residence times are long. These findings do not support reducing or withholding environmental flows. Rather, CH_4 outcomes should be considered alongside ecological, cultural, biodiversity, water-quality, and habitat objectives, with particular attention to flow timing, source-water quality, connectivity, oxygenation, and net flushing.

Overall, the study establishes a regional baseline for aquatic CH_4 emissions and provides a process-based foundation for incorporating CH_4 into climate adaptation, environmental-water management, and future carbon accounting in the CLLMM and comparable flow-managed coastal systems.

Acknowledgements

We acknowledge the cultural connections to the land and connected water for the people of the Ngarrindjeri and Boandik Nations across the Coorong, Lower Lakes, and Murray Mouth region. We recognise that First Nations peoples' spiritual, social, cultural, and economic practices come from their lands and waters, and they continue to maintain their cultural heritage, economies, languages, and laws which are of ongoing importance.

This project was funded by the Goyder Institute for Water Research's CLLMM Research Centre, which is funded by the Australian Government. We thank the CLLMM Research Centre staff (especially Dr Nick Whiterod, Sue Ellison, Jane French, Fiona Adamson, and Dr Alec Rolston) for First Nations consultation support, and project initiation and management. We thank the Goyder Institute for Water Research, Research Advisory Committee and two anonymous reviewers for constructive feedback on the report.

The Authors also acknowledge the sensor calibration, and chamber design support of Dr. Jonas Stage Sø, Professor Theis Kragh, Professor Murray Hamilton, Dr Michael Hatch, and Dr Carolina Trochine.

Glossary

ANME: Anaerobic methane-oxidising microorganisms, which consume methane in the absence of oxygen.

CH_4: Methane, a greenhouse gas with ~80× the warming effect of CO_2 on a 20-year timescale.

Diffusion: The continuous transfer of dissolved methane from one medium to another (in this case from water to the atmosphere).

Ebullition: The episodic release of methane bubbles from sediments through the water column to the atmosphere. Often predominates when there are very high rates of methane production (where production is greater than can be balanced by diffusion alone).

fDOM: Fluorescent dissolved organic matter, an optical proxy for part of the dissolved organic-matter pool.

Groundwater and porewater advection: The movement of methane-rich water from groundwater or sediment pore spaces into the overlying water body.

H1–H6 habitat categories: Salinity-defined habitat categories used in this report, ranging from freshwater or low-salinity conditions in H1 to hypersaline conditions in H6.

Hypersaline: Having a salinity greater than seawater (about 35 PSU depending on local oceanographic factors).

Hypoxia and anoxia: Conditions with very low oxygen and no oxygen, respectively. These conditions can favour methane production and constrain aerobic methane oxidation.

Labile organic carbon: Organic carbon that microorganisms can readily break down and use, more readily stimulating methane production.

Methanogen and Methanogenesis: A microorganism responsible for biogenic methane production, and the process of methane production under anoxic conditions, respectively.

Acetoclastic methanogenesis: Methane production specifically from acetate, a competitive substrate with sulfate-reducing Bacteria.

Hydrogenotrophic methanogenesis: Methane production specifically from CO_2 + H_2, competitive substrates with sulfate-reducing Bacteria.

Methylotrophic methanogenesis: Methane production specifically from methylated compounds, often non-competitive substrates which are abundant in stressful environments as the can help facilitate plant, animal, or microbial survival (examples include: glycine betaine, choline sulfate, trehalose).

Methane flux: The rate at which methane moves between an aquatic environment and the atmosphere, usually expressed per unit area and time.

Methane oxidation: Microbial consumption of methane before it reaches the atmosphere.

Methanotroph: A microorganism that consumes methane through methane oxidation.

PCoA: Principal coordinates analysis, an ordination method used to visualise differences in community composition among samples.

PERMANOVA: Permutational multivariate analysis of variance, used here to test whether microbial community composition differed among habitat categories.

Random forest: A statistical machine-learning method used here to identify environmental variables associated with variation in measured methane flux.

Sulfate-reducing bacteria: Microorganisms that use sulfate rather than oxygen during respiration and can compete with methane-producing microorganisms for substrates in saline sediments.

Water residence time: The average time water remains within a lake, lagoon, or section of a water body before being replaced or exported.

1 Introduction

Coastal lagoons are climate-sensitive ecosystems that can themselves act as important, yet poorly constrained, sources of methane (CH_4; Bonaglia et al., 2025; Keneally et al., 2025b). Methane (CH_4) is a potent greenhouse-gas and a major driver of near-term warming, making it especially relevant to climate adaptation because changes in CH_4 emissions can rapidly influence radiative forcing (IPCC, 2021). Aquatic environments are increasingly recognised as significant methane sources, yet saline and hypersaline coastal lagoons remain underrepresented in the CH_4 datasets informing many global climate models (Bastviken et al., 2004; Villalobos et al., 2025).

Meanwhile, these systems are highly vulnerable to climate change across many coastal regions, facing reduced freshwater inflows, warming-driven evaporation, and sea-level rise, contributing to expected increases in salinisation and altered hydrological connectivity, with important consequences for carbon cycling and greenhouse-gas emissions (Keneally et al., 2025b; Mosley et al., 2023; Rees et al., 2022; Tweedley et al., 2019).

In the Coorong, Lower Lakes and Murray Mouth (CLLMM) region, these issues are magnified. The CLLMM is regulated by freshwater flows, is highly vulnerable to climate forcing, and hosts a Ramsar-listed wetland that has experienced strong hydrological alteration, persistent drying pressure, and increasing salinity stress, while future sea-level rise is expected to further strengthen marine influence on the system (Rees et al., 2022). Understanding CH_4 dynamics in this system is therefore relevant not only to wetland carbon budgets, but also to climate adaptation strategy, and flow-management planning.

Salinity is often expected to suppress methanogenesis because sulfate-rich saline waters favour more energetically efficient anaerobic respiration pathways (sulfate reducing bacteria; SRB), which can outcompete many methanogens for key substrates (Poffenbarger et al., 2011). However, this does not entirely suppress CH_4 production, especially in organic-rich sediments where specialised microbial pathways may persist despite high salinity (Welsh, 2000). In the Coorong, recent work showed that CH_4 production potential can remain substantial in hypersaline depositional sediments, with methylotrophic methanogenesis emerging as an important pathway linked to organic matter accumulation and distinct microbial community structure (Keneally et al., 2025a, 2024b). These findings challenge the simple assumption that increasing salinity uniformly reduces methane production and instead suggest that pathway-specific responses are critical in saline coastal lagoons. Despite this progress, important uncertainties remain regarding how sedimentary methane production translates into atmospheric emissions, particularly the relative roles of diffusive and ebullitive CH_4 flux across steep salinity gradients.

For any given pool of organic carbon within an aquatic system, the eventual atmospheric release of methane reflects the balance among four overarching controls (Figure 1). These are:

- Methanogenesis, the microbial production of CH_4 by methanogenic Archaea under anoxic conditions;
- Methane oxidation, the biological consumption of CH_4 by aerobic and anaerobic methane oxidisers before it reaches the atmosphere;
- Carbon storage or retention, where carbon is diverted away from rapid mineralisation and instead buried in sediments or retained in more stable biomass such as macrophyte tissue; and
- Physical emission controls, which regulate how efficiently CH_4 is transferred from groundwater, sediments, and water to the atmosphere through processes such as diffusion, ebullition, mixing, degassing, and (particularly for saline environments) changes in gas solubility.

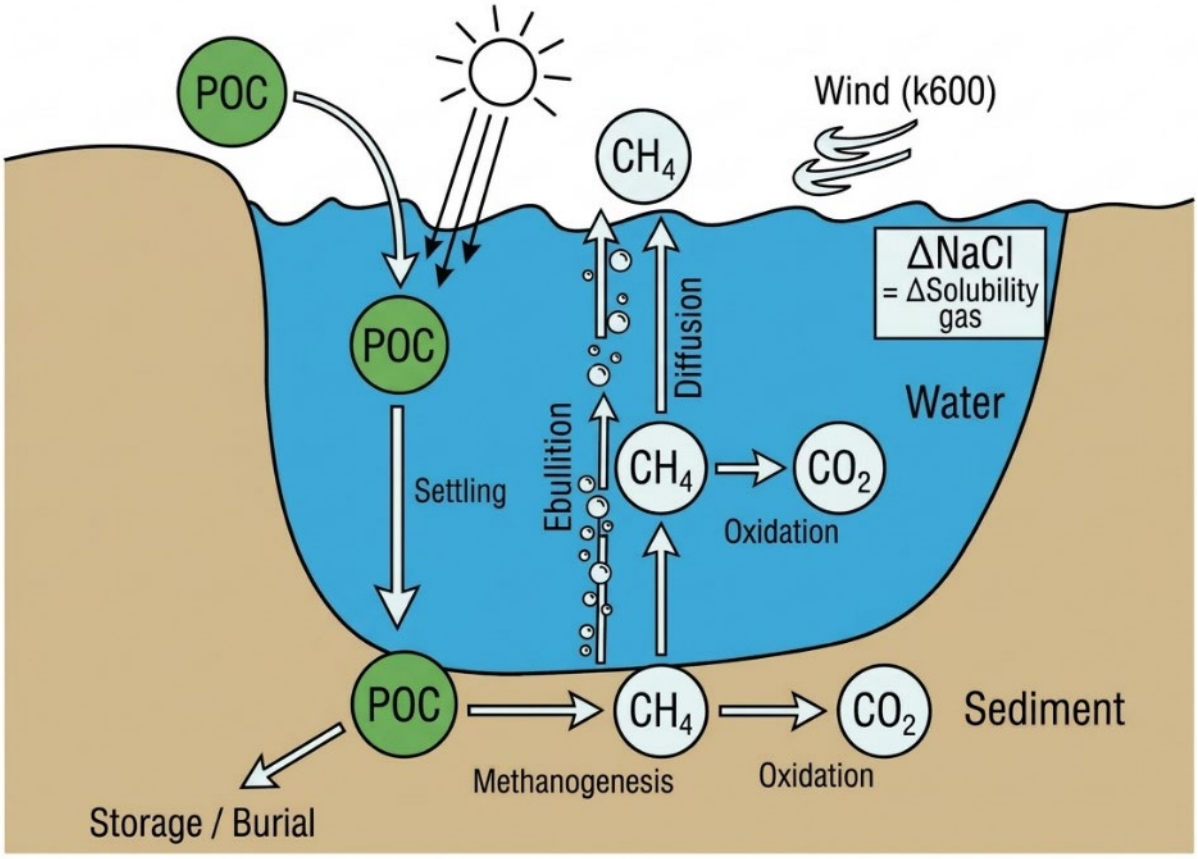

Figure 1. Simplified conceptual model of the four overarching controls on methane (CH_4) emissions in saline aquatic environments. Particulate organic carbon (POC) enters the system from external inputs and in situ production, settles through the water column, and may be buried, or converted to CH_4 in sediments. CH_4 can then be either oxidised or released to the atmosphere via diffusion or ebullition, with rates further influenced by wind-driven gas exchange and salinity-related changes in gas solubility.

Superimposed on these broad controls are pathway-specific mechanisms at the air-water interface, where total flux (F_{total}) is often partitioned into diffusive (F_{diff}) and ebullitive (F_{ebul}) components (Figure 1):

$$F_{total} \approx F_{diff} + F_{ebul} \quad (1)$$

These pathways typically respond quite differently to environmental change, with diffusive emissions often reflecting concentration gradients and turbulence

(MacIntyre, 1995), whereas ebullition is more episodic and influenced by sediment gas accumulation when CH_4 production exceeds sediment-water diffusive loss, hydrostatic pressure driven by water depth (DelSontro et al., 2016; Sø et al., 2025). Resolving the relative contributions of F_{diff} and F_{ebul} to total emissions is therefore essential for robust methane budgets.

Hydrology can further modify each of these four controls by altering salinity, nutrient supply, carbon inputs, residence time, inundation patterns and lateral transport. In flow-regulated systems like coastal lagoons, freshwater inflows can enhance methane production indirectly by delivering labile allochthonous carbon and nutrients (Bonaglia et al., 2025; Chuang et al., 2017; Li et al., 2022; Zhou et al., 2025), while also changing connectivity among habitats and shifting local salinity conditions (Chilton et al., 2021).

Tidal forcing can strongly regulate CH_4 transport and emissions in estuaries by promoting sediment resuspension, porewater exchange, groundwater advection, and the lateral transport of methane-rich water. These processes can increase surface-water CH_4 concentrations and diffusive fluxes, although the magnitude and direction of tidal effects vary among systems (Li et al., 2021; Maglaya et al., 2025; Sadat-Noori et al., 2025; Trifunovic et al., 2020).

Hydrological restriction is also important in coastal wetlands and lagoons because reduced tidal connectivity, longer residence times and weaker flushing can promote organic-matter accumulation, oxygen depletion and prolonged anoxia, thereby favouring methanogenesis and emissions (Bonaglia et al., 2025; Brown et al., 2022). By contrast, stronger marine exchange may suppress CH_4 production by 'flushing-out' labile carbon and nutrients (Keneally et al., 2025a), and by increasing sulfate availability for competitive sulfate-reducing Bacteria (Poffenbarger et al., 2011).

In the CLLMM, these interacting controls are especially relevant because hydrological regulation alters both connectivity to freshwater inflows and the strength of the estuarine-to-hypersaline gradient, creating a natural setting in which salinity and hydrology can be evaluated together rather than as isolated drivers of CH_4 emissions

Here, we use the CLLMM as a natural salinity gradient to ask four questions:

1) how do present salinity and hydrological factors structure the habitat of methane-cycling microorganisms;
2) how do these factors influence CH_4 emissions and the relative importance of diffusion versus ebullition;
3) how do measured (site-based) emissions scale to the wider CLLMM; and
4) how do projected changes in lagoon habitat extent alter the direction and approximate magnitude of CH_4 emissions under future climate scenarios.

By linking microbial habitat, hydrology, salinity, measured fluxes, this study aims to identify likely controls on system CH_4 emissions, and provide a strong process-based foundation for regional monitoring and climate adaptation in the CLLMM, and comparable flow-managed coastal systems.

2 Methods

2.1 Study design & methane-cycling microbial community assessment

Methane-cycling microbial habitat was characterised by combining an existing dataset of surface (upper 5 cm) sediment microbes collected across the Coorong, Lower Lakes and Murray Mouth (CLLMM) during 2019–2022 with an additional targeted campaign in March 2025. The legacy dataset spanned the salinity gradient of the Coorong and included sites from the tidally influenced North Lagoon through to the highly saline South Lagoon, as previously described by Keneally et al., (2026, 2025a, 2024). In March 2025, three additional sediment samples were collected at each of four sites to strengthen habitat representation at key endpoints and transitions of the regional salinity gradient: Lake Albert (LA; freshwater), Goolwa Barrage (GB; tidal-estuarine), Parnka Point (PA; constriction between North and South Lagoon), and Salt Creek (SC; terminal hypersaline South Lagoon). Because microbial and flux sampling were not fully contemporaneous, the 2019–2022 dataset was used to represent recurring salinity-associated habitats rather than microbial conditions during individual flux measurements. The March 2025 campaign provided more recent coverage, although microbial sampling preceded flux monitoring. Microbial data were therefore integrated at the habitat category level rather than as paired predictors of individual chamber observations, allowing broad habitat associations to be identified but not short-term microbial responses during flux deployments.

DNA extraction, amplicon sequencing and primary laboratory procedures followed the same protocols as previously outlined (Keneally et al., 2026, 2025a, 2024a, 2024b). Briefly, sediment DNA was extracted using the DNeasy PowerSoil kit (Qiagen, USA), with extraction blanks included in each batch. DNA concentration was quantified using a Qubit fluorometer (Thermo Fisher Scientific). The V3–V4 region of the 16S rRNA gene was amplified using primers 341F (5′-CCTAYGGGRBGCASCAG-3′) and 806R (5′-GGACTACNNGGGTATCTAAT-3′), widely used for broad prokaryotic coverage, and indexed amplicons were sequenced on an Illumina MiSeq platform using 2 × 300 bp chemistry.

For downstream integration with flux modelling, microbial samples were assigned to six salinity-defined habitat categories using measured salinity (PSU), following the thresholds implemented in Chilton et al., (2026): H1 = 0–4, H2 = 5–20, H3 = 21–40, H4 = 41–84, H5 = 85–119 and H6 ≥ 120. These categories provided a finer habitat stratification than the broader estuarine/intermediate/hypersaline classes used to analyse this data previously (Keneally et al., 2026).

Table 1. Methane-cycling microbial habitat sampling sites included in the integrated analysis.

CODE	SITE	GENERAL SETTING	N SAMPLES (112 TOTAL)	NOTES
GB	Goolwa Barrage	Tidal-estuarine / barrage outflow interface	3	Added in March 2025 sampling
JP	Jack Point	Hypersaline/ South Lagoon	6	Existing dataset
LP	Long Point	Brackish / North Lagoon	17	Existing dataset
NM	Noonamena	Brackish / North Lagoon	3	Existing dataset
PA	Parnka Point	Hypersaline / Transition – South Lagoon	8	Sampled in existing dataset and in March 2025
PP	Policemans Point	Hypersaline / South Lagoon	14	Existing dataset
SC	Salt Creek	Hypersaline / South Lagoon	16	Sampled in existing dataset and in March 2025
SPT	Snipe Point	Hypersaline / South Lagoon	15	Existing dataset
VDY	Villa Dei Yumpa	Hypersaline / South Lagoon	16	Existing dataset
WW	Woods Well	Hypersaline / South Lagoon	12	Existing dataset
LA	Lake Albert	Freshwater Lake	3	Added in March 2025 sampling

Note: "Samples" refer to separate biological replicates, where intra-core subsamples are combined *in silico* to address within-sample microbial community heterogeneity.

2.2 Chamber-based CH_4 measurements

Water-air CH_4 fluxes were quantified at GB, PA, LA, and SPT (Table 1) every 2 months from May 2025 – January 2026, using a set of 6 autonomous CH_4 sensors (Sø et al., 2024), housed within floating chambers (Figure 2). During each deployment, the chambers were tethered in a line to an anchored buoy and separated by approximately 2 m of rope. Chambers could move freely around the buoy, providing spatial replication within the deployment area. Measurements were collected over a minimum of three automated cycles, each comprising 40 min of headspace sampling, followed by 20 min of flushing with ambient air. This produced at least 18 chamber-cycle measurements per site and deployment: six spatially replicated chambers measured over three repeated cycles. Although this design captured site-level variability, it may not fully represent fine-scale spatial heterogeneity.

Sensor and chamber platforms were assembled following the general design philosophy of Bastviken et al., (2020), and the automated chamber approach of Sø et al., (2024). This configuration was selected because the extreme salinity of parts of the Coorong poses a substantial corrosion and failure risk to high-cost cavity-ring-down or off-axis analysers during prolonged field deployment. Each logger contains a metal-oxide semiconductor CH_4 sensor (Figaro, Japan; NGM2611-E13) and a co-located temperature and relative humidity sensor (Sensirion, Switzerland; SHT45). These were mounted in the top of floating chambers with a chamber volume of 20 L (0.02 m^3) and water-contact area of 0.07 m^2 (Figure 2). The chamber headspace was automatically

vented between measurement intervals, enabling repeated high-frequency measurements and partitioning of diffusive and ebullitive emissions. Before field-collected NGM2611-E13 sensor data could be converted to CH_4, the sensors were first calibrated under controlled laboratory conditions.

Figure 2. Floating chambers deployed and measuring CH_4 fluxes at Parnka Point, Coorong SA.

2.2.1 Sensor calibration

A two-step laboratory calibration was used. First, a humidity-background calibration quantified the change in baseline sensor voltage with changing absolute humidity. Relative humidity (RH, %) and sensor temperature (T, °C) were converted to absolute humidity (ppmv) using the saturation vapour pressure relationship:

$$P_{ws} = A \times 10^{\left(\frac{mT}{T+Tn}\right)} \quad \textbf{(2)}$$

$$H_2O_{ppm} = \frac{RH}{100} \times \frac{P_{ws}}{p} \times 10^6 \quad \textbf{(3)}$$

where P_{ws} is saturation vapour pressure, P is ambient pressure, and A, m, and Tn are empirical constants (Buck, 1981). The humidity-dependent zero-offset voltage was then estimated as:

$$V_0 = gH + P \quad \textbf{(4)}$$

where V_0 is the humidity-adjusted baseline sensor voltage, H is absolute humidity (ppmv), and g and P are fitted calibration coefficients. Second, the humidity-corrected resistance ratio of the sensor was calculated as:

$$\frac{R_S}{R_0} = \frac{(Vc/V)-1}{(Vc/V_0)-1} \quad \textbf{(5)}$$

where V is measured sensor voltage and Vc is the circuit voltage (5,000 mV). Calibrated CH_4 concentrations were then predicted using a nonlinear model with humidity interaction (Bastviken et al., 2020):

$$CH_4 = a\left(\frac{R_S}{R_0}\right)^b (1 + cH_k) + K \quad \textbf{(6)}$$

where $H_k = H_2O\ ppm/1000$, and a, b, c, and K are fitted coefficients. Calibration coefficients were fitted against empirical measurements of known CH_4 concentration simultaneously measured on a Picarro G2201i (Picarro, USA) isotopic CH_4 reference analyser and then applied to independent field datasets to generate final chamber headspace concentrations. Bastviken et al., (2020) showed this approach provides robust accuracy across a range of approximately 2–700 ppm CH_4, which matches the intended sensor range used in the present study.

2.2.2 Flux calculation

Chamber deployments were divided into measurement blocks separated by >10 min gaps. Within each block, the rate of change in calibrated headspace CH_4 concentration was estimated by linear regression of concentration against elapsed time. Flux was then calculated from the ideal gas law as:

$$F = \frac{dC}{dt} \times \frac{V}{A} \times \frac{P}{RT} \quad \textbf{(7)}$$

where F is flux (μmol m^{-2} h^{-1}), dC/dt is the chamber headspace concentration change rate (ppm s^{-1}), V is chamber volume (m^3), A is chamber footprint area (m^2), P is mean chamber pressure (Pa), R is the universal gas constant, and T is mean chamber air temperature (K). Hourly fluxes were calculated directly from fitted block-wise slopes and later converted to daily fluxes for statistical analysis.

Diffusive and ebullitive pathways were separated using the running-variance approach described in Sø et al., (2024). Running variance was calculated from the five most recent CH_4 observations, and ebullition events were identified when variance exceeds a threshold, using default *FluxSeparator* settings (*runvar_cutoff*: 0.5). F_{ebul} was then calculated from the summed concentration increments attributable to bubbles during each measurement cycle, while F_{diff} was estimated after excluding those ebullitive segments and fitting the remaining monotonic increase in headspace CH_4 concentrations. Finally, total fluxes were calculated as $F_{diff} + F_{ebul}$, as defined in equation 1.

2.3 Physicochemical and biological metadata measurement

Water-column physicochemical data were compiled from a combination of *in situ* measurements and external monitoring records. *In situ* variables included salinity, water temperature, dissolved oxygen, pH, chlorophyll-*a* and fluorescent dissolved organic matter (FDOM), measured during flux sampling with a YSI EXO 3 multiparameter probe (Yellow Springs Instruments, USA). Wind speed and barrage-flow data were obtained from the South Australian government Water Data portal (water.data.sa.gov.au), using the nearest available station or barrage record relevant to each site, date, and time. Sediment organic matter (OM) was measured from the upper 0–40 mm of sediment cores collected during March campaigns. Approximately 12 g aliquots were dried at 60°C to constant mass and combusted at 550°C to constant mass; sediment organic matter (%) was calculated as loss on ignition relative to dry mass, and mean values were taken for each site. These variables were used as candidate predictors in the flux screening and predictive models because earlier Coorong work has already shown that salinity, temperature, pH, and sediment organic content structure microbial habitat across the system (Keneally et al., 2024b).

2.4 Statistical analysis

All statistical analyses were run in R (version 4.4.0; R Core Team, 2021). Flux analyses focused on daily CH_4 fluxes (F_{CH4} mg m^{-2} d^{-1}). First, predictors were ranked by the strength of their overall linear association with CH_4 flux. The workflow then generated ordinary least-squares fits for the overall dataset and, where supported by sufficient data, separately for diffusion-only and ebullition-only subsets. These exploratory regressions were repeated overall and within salinity category, habitat category, season, site and region.

Random-forest modelling was then used to quantify the importance of continuous predictors for two purposes: (i) prediction of CH_4 flux across the CLLMM, and (ii) discrimination among habitat categories (H1–H6) based on methane-cycling microbial data. For continuous flux models, predictors with zero variance or no finite values were excluded; remaining numeric predictors were median-imputed and normalised within a *tidymodels* recipe. Data were split 80:20 into training and holdout sets. Models were tuned using five-fold cross-validation on the training data, with *mtry* and *min_n* optimised over a grid of 25 parameter combinations and 1,000 trees per model. Final model performance was evaluated on the holdout dataset using RMSE, MAE and R^2. Variable importance was estimated using permutation importance in ranger (Wright and Ziegler, 2017), bootstrapped 200 times within the training set, and summarised as bootstrap mean importance ± SD. Accumulated local effects were examined for the top predictors to aid interpretation of fitted relationships where predictors were potentially correlated.

Random forests are well suited to identifying non-linear and interacting environmental controls on CH_4 flux (Breiman, 2001), and the ranger implementation provides efficient permutation-based variable importance estimation (Wright and Ziegler, 2017). Given the limited spatiotemporal coverage, model outputs were interpreted here as

exploratory associations and directional relationships rather than as robust forecasts for unsampled locations or future periods.

Microbial community analyses were conducted on an explicitly filtered methane-cycler subset. The workflow imported and merged QIIME2 objects into *phyloseq* (McMurdie and Holmes, 2013), removed chloroplast and mitochondrial reads, and standardised metadata fields for site, salinity-defined habitat category, season, and month. Beta-diversity was then assessed using Bray–Curtis dissimilarity on relative-abundance data and visualised using PCoA ordination. Community differences among the salinity-defined habitat categories (H1–H6) were tested using unconstrained PERMANOVA, with 999 permutations.

Methane-cycling taxa were identified using explicit taxonomy-based filtering of known methanogenic and methane-oxidising taxa. Candidate methanogens were matched at Genus-, Family- or Order-level annotations and included taxa such as Methanofastidiosales, Methanomassiliicoccales, *Methanolobus*, *Methanococcoides*, *Methanogenium*, *Methanosarcina*, *Methanohalobium* and *Methanohalophilus*. Candidate aerobic methane oxidisers included *Methyloceanibacter*, *Methylophaga*, *Methylotenera*, *Methyloligellaceae*, *Methylohalomonas*, *Methylohalobium*, *Methylacidiphilaceae* and related methylotrophic groups. Anaerobic methanotrophs were identified separately by matching ANME-designated taxa and *Methanoperedenaceae*. Retained taxa were then collapsed into four functional groups using flexible taxonomy matching across available ranks: (i) methylotrophic methanogens, (ii) acetoclastic/hydrogenotrophic methanogens, (iii) aerobic methane oxidisers, and (iv) anaerobic methanotrophs (ANMEs). Functional-group abundance for each sample was calculated as the summed count of all taxa assigned to each group.

Habitat discrimination by methane-cycling communities was assessed using random-forest classification implemented in ranger, with functional-group relative abundances as predictors and habitat category (H1–H6) as the response. Variable importance was quantified as bootstrap mean permutation importance ± SD, consistent with the continuous CH_4-flux random-forest models. For visualisation, functional-group relative abundance was averaged within each habitat category, log-transformed with a small pseudocount, and standardised within each functional group as row-wise z-scores across H1–H6, so that heatmaps represent relative enrichment or depletion along the salinity gradient rather than absolute abundance.

Due to limited habitat category data, future CH_4 emissions under climate scenarios were projected for the Coorong Lagoons and did not include the Lower Lakes. Briefly, CH_4 flux was first estimated for each salinity-defined habitat category, and these habitat-specific emission factors were then combined with scenario-based changes in habitat extent under projected warmer and drier conditions (as detailed in Vang et al., 2026, Chilton et al., 2026). Total future emissions were calculated by multiplying habitat-specific mean flux by the projected area of each habitat and summing across habitats. Projected emissions were summarised as mean values ± standard error.

3 Results

3.1 Methane-cycling microbial communities

Methane-cycling microbial communities varied significantly among habitat categories, indicating compositional turnover across the salinity gradient (Figure 3; R^2: 0.18; p <0.001). Ordination of the filtered methane-cycler subset showed clear compositional separation across the freshwater to hypersaline gradient, indicating that, while most variance remains unexplained by the PERMANOVA model, habitat category is a key determinant of methane-cycling assemblages in the CLLMM.

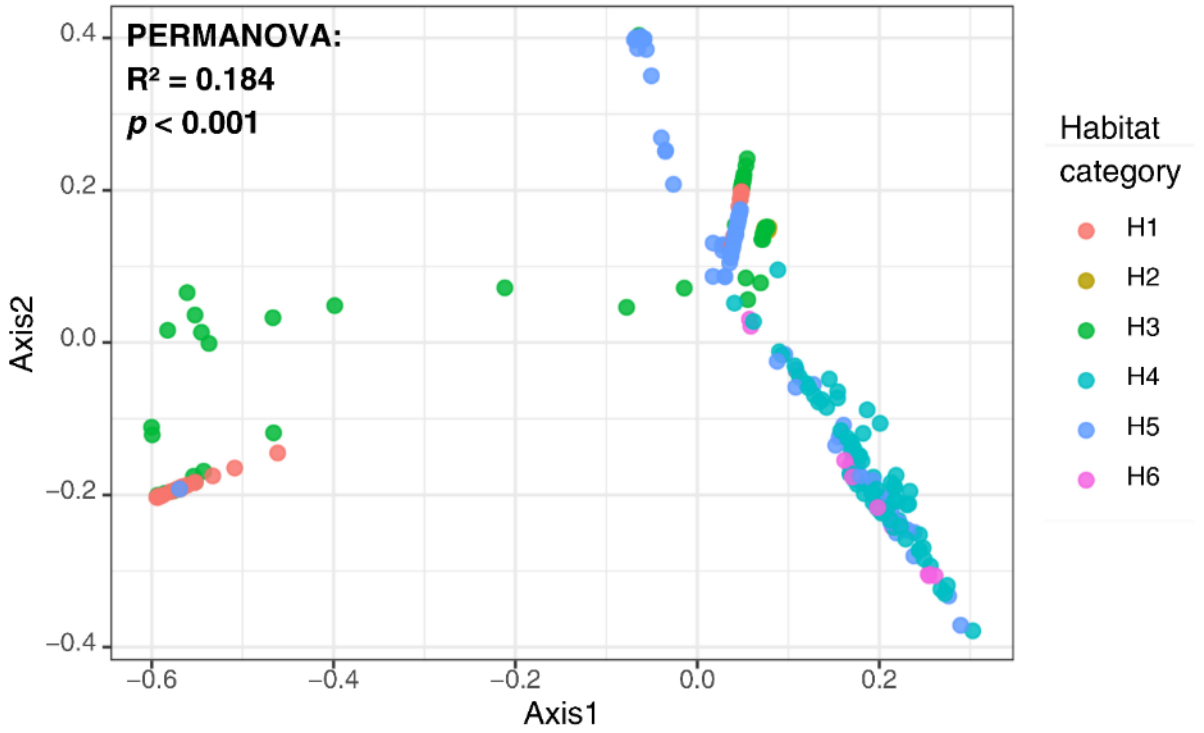

Figure 3. Principal coordinates analysis (PCoA) of methane-cycling microbial community composition based on Bray–Curtis dissimilarity of relative abundances. Points represent individual samples coloured by salinity-defined habitat category (H1–H6).

The random-forest classification identified an additional habitat-associated signal in methane-cycling community composition across the salinity gradient (Figure 4). When taxa were grouped by metabolic function, aerobic CH_4 oxidisers and methylotrophic methanogens emerged as the most important discriminators of habitat category, followed by acetoclastic/hydrogenotrophic methanogens and ANMEs (Anaerobic Methane Oxidisers).

Aerobic methane oxidisers, represented by taxa such as *Methyloceanibacter spp.*, *Methylophaga spp.*, *Methylotenera spp.* and related methylotrophic lineages, were relatively enriched in fresher to moderately saline habitats, consistent with greater potential for aerobic CH_4 consumption in these zones. In contrast, methylotrophic methanogens, including Methanofastidiosales, Methanomassiliicoccales, *Methanolobus spp.*, *Methanococcoides spp.*, and *Methanohalophilus spp.*, were more strongly associated with higher-salinity habitats, indicating a potential shift

towards methylotrophic methane production pathways under saline to hypersaline conditions. This pattern is consistent with increasing evidence that methylotrophic methanogenesis can remain active, and in some settings dominate, where classical acetoclastic or hydrogenotrophic pathways are constrained (Nobu et al., 2016), and accords with previous Coorong sediment studies implicating methylotrophic methanogenesis in hypersaline depositional zones (Keneally et al., 2024b). More broadly, these functional-group patterns suggest greater relative enrichment of methane-producing groups in higher-salinity habitats, alongside weaker representation of aerobic methane oxidisers, suggesting reduced CH_4 biofiltration under hypersaline conditions (H5; Figure 4).

Acetoclastic/hydrogenotrophic methanogens and ANMEs also varied across habitat categories but contributed less strongly to discrimination among habitats than the aerobic methane oxidisers and methylotrophic methanogens. Together, these results indicate that salinity-defined habitat transitions may reorganise methane-cycling communities at the functional level, with potential implications for the balance between CH_4 production and oxidation across the CLLMM.

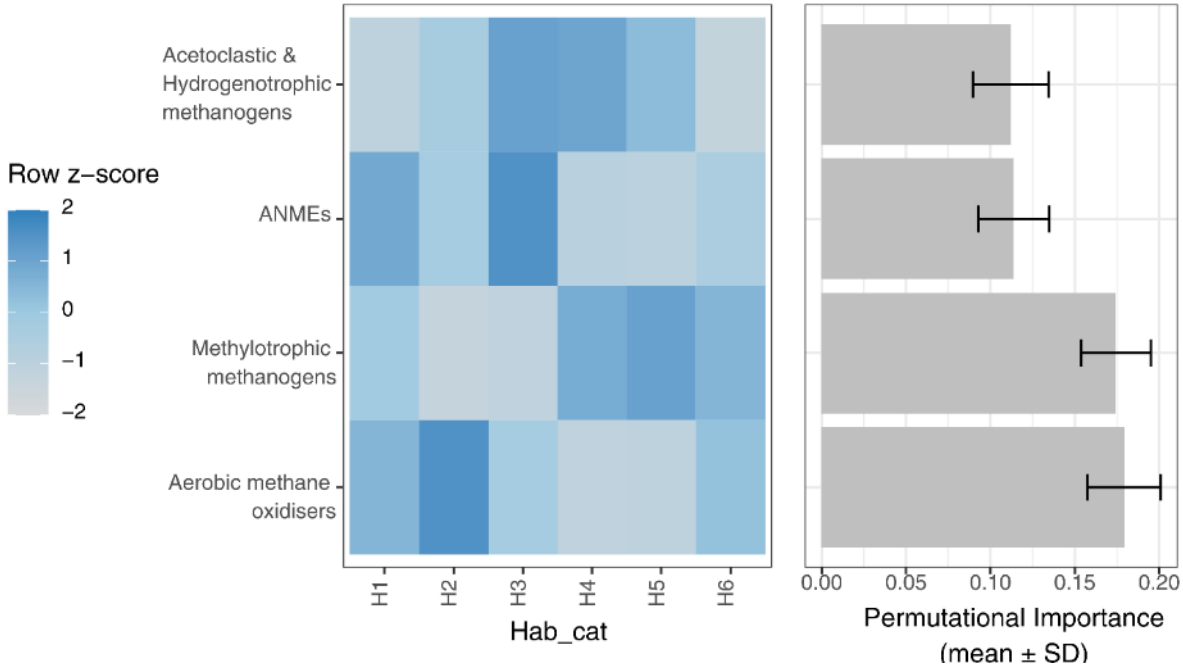

Figure 4. Functional-group patterns in methane-cycling communities across habitat categories. The heatmap shows row z-scores of log-transformed mean relative abundance for four methane-cycling functional groups across salinity-defined habitat categories (H1–H6), where darker shading indicates relative enrichment within a given habitat. The paired bar plot shows bootstrap mean permutation importance (± SD) from the random-forest model used to discriminate important methane-cycling functional groups across habitat categories.

3.2 Predictors of CLLMM CH_4 fluxes

CH_4 fluxes varied strongly among sites and pathways, with ebullition observed only in low salinity waters (<1 PSU), whereas diffusive fluxes occurred across the full salinity gradient. Linear analyses identified tide height, water temperature, sediment organic matter, dissolved oxygen (DO), total barrage flows, and total dissolved solids (TDS; salinity) as the six strongest predictors of flux (Figure 5). Among these, tide height was the strongest linear predictor of diffusive flux, explaining a substantial proportion of variance (R^2: 0.38; $p < 0.001$; Figure 5). This indicates that short-term hydrodynamic forcing is a key control on CH_4 exchange in the system, likely via changing water depth, hydrostatic pressure, connectivity, and advection of CH_4-rich waters. Similar tidal regulation of estuarine CH_4 concentrations and fluxes has been reported elsewhere, although the direction and magnitude of the effect vary among systems (Li et al., 2021; Trifunovic et al., 2020).

Water temperature showed contrasting relationships among pathways, being positively associated with ebullitive flux but negatively associated with diffusive flux overall. This likely reflects the stronger influence of hydrology and seasonality on net CH_4 emissions in the CLLMM. Although methanogenesis typically increases with temperature (Yvon-Durocher et al., 2014), higher CH_4 fluxes here also coincided with periods of greater freshwater inflow, which may deliver labile carbon and stimulate methane production even under cooler conditions. The positive association between temperature and ebullition is also consistent with enhanced bubble formation and release in shallow freshwaters, although the patchiness of ebullition adds uncertainty to this relationship.

Sediment organic matter was a strong positive correlate of both ebullitive and diffusive flux, consistent with the role of organic-rich depositional sediments as methane-production hotspots in the Coorong and in coastal lagoons more broadly (Keneally et al., 2024b; Bonaglia et al., 2025).

Contrary to simple salinity-suppression paradigms informing some coastal carbon management (e.g. Poffenbarger et al., 2011), diffusive CH_4 fluxes persisted across the hypersaline gradient and did not decline monotonically with salinity. Indeed, the highest-emitting habitat category occurred at high salinity (H5), indicating that salinity alone does not determine net CH_4 emissions.

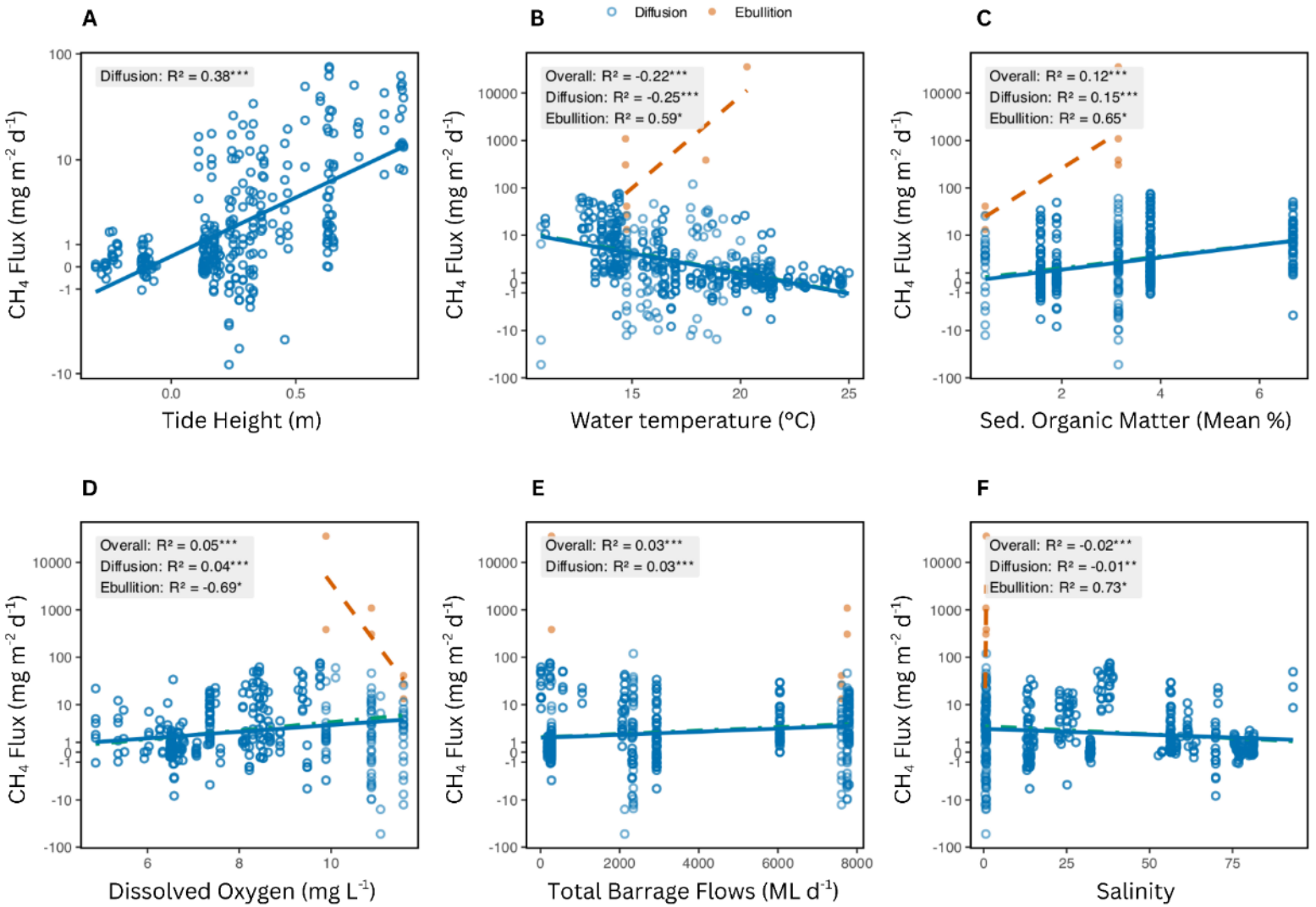

Figure 5. Linear relationships between predictors & CH_4 flux. Panels show relationships with the six strongest linear predictors. Points are individual flux observations, coloured by pathway (diffusion: blue, ebullition: orange). Fitted lines are shown where relationships were significant, with an additional green dash-dot line (primarily traces the diffusion line) representing significant summed fluxes from both pathways. Asterisks denote significance: $p < 0.05$ *, $p < 0.01$ **, $p < 0.001$ ***. Abbreviations: Sed. = Sediment.

Within the measured dataset, random-forest models highlighted dissolved organic matter fluorescence (fDOM), tide height, DO, turbidity, water temperature, and total barrage flows as the most informative environmental predictors of CH_4 flux at the whole-system scale (Figure 6). In these models, hydrological and physicochemical predictors outweighed temperature alone, indicating that system connectivity, water-column condition, and organic-matter proxies jointly structure emissions more strongly than any single climatic variable. Holdout performance was modest (R^2: 0.22, MAE: 4.213, RMSE: 7.96 mg CH_4 m^{-2} d^{-1}). The model is therefore useful for identifying likely controls and directional structure but does not provide sufficiently strong predictive skill for robust forecasting at unsampled locations or future times.

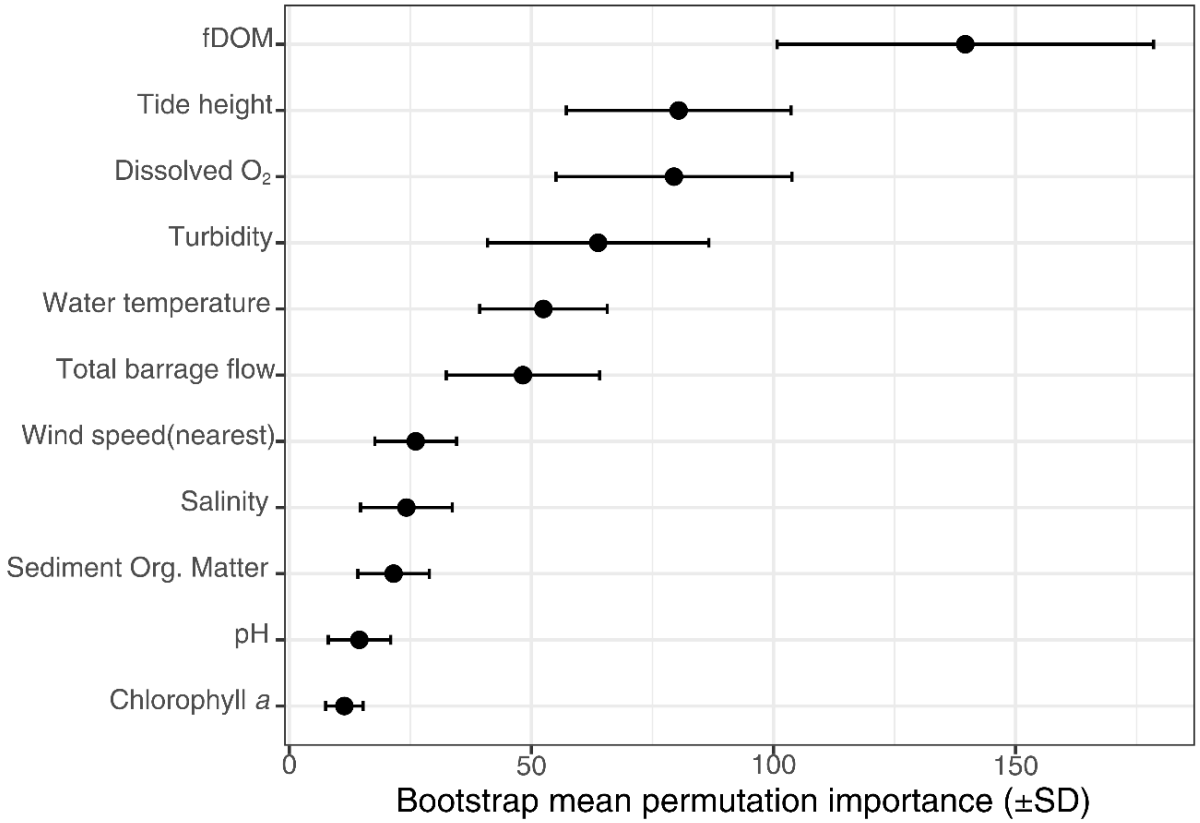

Figure 6. Random-forest variable importance for explaining variation in CLLMM CH_4 flux. Bars show bootstrap mean permutation importance (± SD) for the strongest environmental predictors. Abbreviations and units: fDOM (Fluorescent dissolved organic matter; QSU), Tide height (m), Dissolved oxygen (mg L^{-1}), Turbidity (NTU), Water temperature (°C), Total barrage flows (ML d^{-1}), Wind speed at the nearest meteorological station (km h^{-1}), Sediment organic matter (average %), Chlorophyll *a* (RFU).

3.3 *Habitat-informed climate scenario estimates of Coorong CH_4 emissions*

Indicative habitat-informed estimates suggested that CH_4 emissions from the Coorong may increase under hotter, drier future conditions, with the highest projected emissions under the dry and sea-level-rise dry scenarios, whereas median sea-level rise scenarios produced only slight reductions in estimated lagoon emissions (Figure 7). These estimates combine habitat-specific mean fluxes with scenario-based changes in habitat extent and should therefore be interpreted as directional comparisons among scenarios rather than forecasts of future emissions. Uncertainty remains high because of limited spatial and seasonal flux coverage, within-habitat heterogeneity, the episodic nature of ebullition, and uncertainty not represented in the scenario habitat areas.

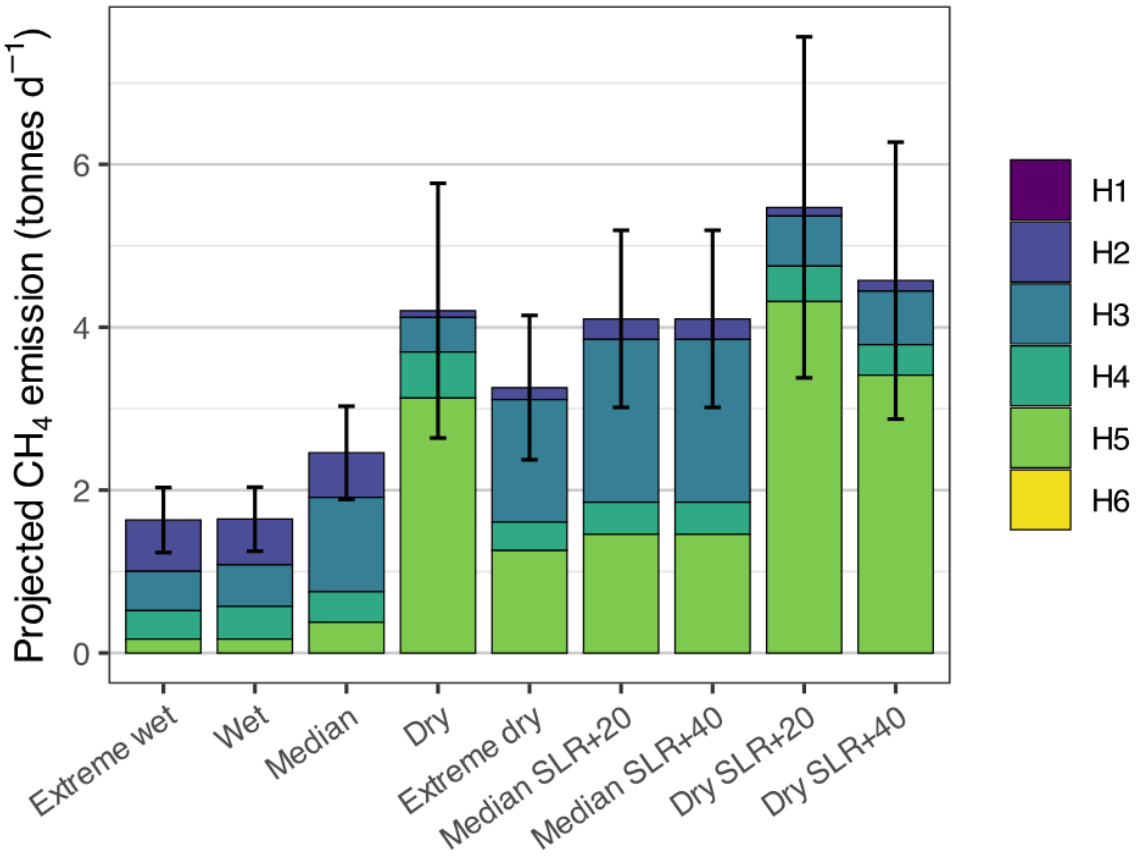

Figure 7. Habitat-informed estimates of total Coorong lagoon CH_4 emissions under future hydrological and sea-level rise (SLR) scenarios. Stacked bars show the contribution of each habitat category (H1–H6) to projected whole-of-system emissions, with error bars indicating total mean ± standard error.

4 Discussion

This study combined microbial habitat assessments, direct chamber-based methane (CH_4) flux measurement, and habitat-informed estimates of future climate scenarios to examine CH_4 emissions across an iconic and critically endangered Australian wetland system. Methane-cycling microbial communities varied significantly with salinity-defined habitat, ebullition was largely confined to freshwaters, and diffusive CH_4 emissions persisted across the full salinity gradient, including hypersaline habitats. Hydrological and organic-matter-related variables, especially tide height, fDOM, organic matter content, dissolved oxygen, and barrage flows, were each more informative of CH_4 emissions than salinity alone. Together, these results show that the CLLMM cannot be interpreted through a simple framework of salinity-driven CH_4 suppression. Instead, CH_4 emissions reflect interacting controls on production, oxidation, storage and physical release, each mediated by habitat, hydrology and substrate availability.

4.1 Salinity structures methane-cycling habitat, but does not simply suppress CLLMM emissions

The clear separation of methane-cycling communities among habitat categories supports the idea that salinity is a major environmental filter in the CLLMM, consistent with previous Coorong studies and broader work on hypersaline lagoons (Keneally et al., 2026, 2024b). However, the flux results show that this habitat filtering does not translate into a simple monotonic suppression of net CH_4 emission. Ebullition was restricted to low salinity waters, in agreement with recent evidence that salinity strongly suppresses ebullitive CH_4 release in lentic waters, where CH_4 production is limited compared to sediment diffusion (Soued et al., 2024).

At the same time, diffusive CH_4 fluxes persisted across the salinity gradient, and the highest-emitting habitat category occurred at high salinity. This is consistent with the idea that salinity suppression can be compensated by abundant organic matter, where specialised pathways remain active (Soued et al., 2024), or where water-residence times are high (Sadat-Noori et al., 2025). In the Coorong, depositional sediments, and high organic loading support methylotrophic methanogenesis and methane production potential even under hypersaline conditions (Keneally et al., 2024b). The relative enrichment of methylotrophic methanogens observed in habitat category H5 aligns with this mechanism, because this functional group is associated with methylotrophic methanogenesis and is increasingly recognised as important in organic-rich, anoxic environments (Nobu et al., 2016; Keneally et al., 2024b).

4.2 Organic matter and hydrology appear to override simple salinity effects

The results suggest that hydrology and organic-matter supply can modify or override simple salinity controls on CH_4 emissions. Tide height was the strongest linear correlate of diffusive flux, while fDOM, dissolved oxygen, turbidity, water temperature, and

barrage flows were the most informative random-forest predictors. Rather than acting as independent causal controls, these variables likely integrate broader patterns of hydrological connectivity, organic-matter transport, and water residence time.

Tidal and water-level variation may alter hydrostatic pressure, sediment–water exchange, and the lateral transport of methane-rich water (Pfeiffer-Herbert et al., 2019). Barrage flows and episodic flushing may further influence organic-matter delivery, oxygen conditions, residence time, and the retention or export of dissolved CH_4 (Brown et al., 2024). Groundwater and porewater advection could provide yet another pressure-sensitive CH_4 source (Maglaya et al., 2025; Sadat-Noori et al., 2025), particularly where fresher groundwater lenses occur beneath the margins of the South Lagoon (Priestley et al., 2022).

Tide height and barrage flow should therefore be interpreted as indicators of broader hydrological connectivity and transport processes. Because groundwater inputs, sediment exchange, and dissolved-gas transport were not measured directly, these mechanisms remain process-based interpretations requiring targeted experimentation and measurement.

4.3 Methane oxidation may be an important, but vulnerable, control on net emissions

The relative abundance of aerobic methane oxidisers declined from H3 towards more saline habitat categories. This included *Methyloceanibacter* lineages, members of which have been demonstrated to oxidise CH_4 in marine sediment and water-column environments (Vekeman et al., 2016; de Groot 2025). The observed pattern suggests a change in methanotrophic community composition across the CLLMM's mid-salinity ranges, and could help explain why diffusive CH_4 emissions persist even where ebullition is suppressed.

Another possible mechanism is inhibition of methane oxidation under the sulfide-rich conditions persisting in the South Lagoon (Keneally et al., 2024b; Mosley et al., 2023, 2022). Hydrogen sulfide can inhibit aerobic methane oxidation and respiration, although some methanotrophs possess adaptations that allow simultaneous sulfide and methane oxidation (Dalcin Martins et al., 2024). In degraded sediments of the Coorong, where sulfide and monosulfidic black ooze readily occur, suppression of methane oxidation by sulfide exposure is therefore a plausible mechanism that warrants direct future testing.

4.4 Implications for climate adaptation and regional management

The CLLMM is already a focus of environmental-water management and climate-adaptation planning, making interactions among flow, water quality, habitat condition, and CH_4 emissions directly relevant to regional decision-making (Dunlop et al., 2022; Rees et al., 2022).

The results of this study indicate that hydrological interventions may have multiple and sometimes opposing effects on CH_4 cycling. For example, during the 2022–23 flood,

nutrient concentrations declined, sediments became better oxygenated, and CH_4-production pathways were depleted, aligning with conclusions here that freshening and flushing can suppress CH_4 accumulation, and enhance CH_4 oxidation (Keneally et al., 2025a). Conversely, inflows rich in nutrients or labile organic carbon may stimulate subsequent CH_4 production, particularly where residence times are long or flushing is limited (Beaulieu et al., 2019; Chilton et al., 2021; Keneally et al., 2024b).

These findings do not support reducing or withholding environmental flows, which remain central to established ecological and water quality objectives (Chilton et al., 2021; Mosley et al., 2023). Rather, CH_4 responses are likely to depend on flow timing, source-water quality, connectivity, oxygenation, residence time, and net flushing.

Likewise, future sea-level rise may slightly reduce lagoon CH_4 emissions through stronger marine influence (Rees et al., 2022), but this does not imply that salinisation is a desirable mitigation pathway, especially given its ecological costs and the observed persistence of diffusive emissions under hypersaline conditions.

The central management challenge for the CLLMM is therefore not to simply minimise salinity, nor to maximise marine exchange, but to manage the system in ways that reduce the build-up and mobilisation of labile carbon and nutrients while maintaining ecological function. In this respect, CH_4 emissions should be carefully considered alongside ecological, cultural, water quality, biodiversity, and habitat objectives when assessing future infrastructure, flow manipulation, or mouth-management scenarios (Dunlop et al., 2022; Mosley et al., 2023).

4.5 Limitations and future work

The upscaled, habitat-based projections captured broad patterns but retained high levels of uncertainty, especially for scenario-based estimates. Flux measurements were collected at relatively few sites over approximately one annual cycle and cannot represent the full spatial and interannual variability of the CLLMM. Furthermore, the microbial analysis presented here was not contemporaneously paired to flux measurements, therefore providing only habitat-level context rather than direct measurement of communities responsible for each observed flux. Finally, habitat and sea-level-rise scenario estimates made here were restricted to the Coorong lagoon section of the CLLMM, and featured very high uncertainty. These emissions estimates should therefore be treated as directional comparisons, not forecasts.

More robust regional estimates will require greater sampling effort targeting warmer freshwater conditions, where ebullition is likely to be more frequent and spatially heterogeneous, and may substantially alter the strength and form of the correlations observed here. Additional flux sampling, with paired assessments of microbial communities, during hotter periods, and under more extreme salinity conditions would therefore improve both empirical and scenario-based flux estimates. More direct measurements of dissolved CH_4, oxidation rates, porewater chemistry, sulfide exposure and sediment redox structure are also needed to resolve the mechanisms linking habitat, microbial composition and net emissions.

5 Recommendations

The findings of this report support the following management and monitoring recommendations:

5.1 Reduce nutrient and labile carbon loads

The results of this study align with previous work (Keneally et al., 2024b), indicating that organic matter supply is a major control on greenhouse-gas emissions, offsetting expected salinity suppression. Management should continue to focus on securing environmental flows to the CLLMM, but focus more on the quality of that water. For example, particular focus should be placed on catchment management to reduce nutrient-rich run-off that can stimulate phytoplankton production and subsequent delivery of labile autochthonous carbon to the Coorong.

5.2 Maintain or restore conditions that support methane oxidation

The decline in methanotrophic taxa across parts of the salinity gradient suggests that methane oxidation may be a vulnerable control on greenhouse-gas emissions. Management actions that reduce hypoxia and sulfide build-up in surface sediments and bottom waters will help preserve this CH_4 biofilter.

5.3 Do not assume that greater salinity or marine intrusion will automatically reduce methane emissions

Ebullition was observed only in low-salinity waters, but diffusive emissions persisted across the entire salinity gradient, where the highest habitat-specific mean occurred at high salinity. Some sea-level-rise scenarios produced small reductions in indicative lagoon emissions, but these estimates remain uncertain and do not support salinisation as a methane-mitigation strategy.

5.4 Expand monitoring to improve carbon budgeting

Future greenhouse-gas monitoring should include broad seasonal coverage, including more high-salinity and high-temperature sampling, and direct measurements of dissolved CH_4, sulfide, oxygen microprofiles, and methane oxidation rates. This will be essential for developing a robust whole-of-system carbon budget and for reducing uncertainty in climate-adaptation planning.

6 References

Bastviken D, Cole J, Pace M, and Tranvik L (2004). Methane emissions from lakes: dependence of lake characteristics, two regional assessments, and a global estimate. *Global Biogeochemical Cycles*, 18, GB4009.

Bastviken D, Nygren J, Schenk J, Parellada Massana R, and Duc NT (2020). Facilitating the use of low-cost methane (CH 4) sensors in flux chambers–calibration, data processing, and an open-source make-it-yourself logger. *Biogeosciences*, 17, 3659–3667.

Beaulieu JJ, DelSontro T, and Downing JA (2019). Eutrophication will increase methane emissions from lakes and impoundments during the 21st century. *Nature Communications*, 10, 1375.

Bonaglia S, Cheung HLS, Politi T, Vybernaite-Lubiene I, McKenzie T, Santos I and Zilius M (2025). Eutrophication and urbanization enhance methane emissions from coastal lagoons. *Limnology and Oceanography Letters*, 10, 140–150.

Breiman L (2001). Random forests. *Machine Learning*, 45, 5–32.

Brown AM, Bass AM, and Pickard AE (2022). Anthropogenic-estuarine interactions cause disproportionate greenhouse gas production: A review of the evidence base. *Marine Pollution Bulletin*, 174, 113240.

Brown AM, Bass AM, White S, Corr M, Skiba U, MacDonald JM, and Pickard AE (2024). The impact of estuarine flushing on greenhouse gases: a study of the stratified Clyde estuary. *Estuarine, Coastal and Shelf Science*, 304, 108830.

Buck AL (1981). New equations for computing vapor pressure and enhancement factor. *Journal of Applied Meteorology and Climatology*, 20, 1527–1532.

Chilton D, Brookes J, Hipsey M, Jamieson T, Keneally C, Waycott M, and Leterme SC (2026). Shifts in flow and salinity shape phytoplankton communities in the Coorong, a Ramsar-listed shallow coastal lagoon (South Australia). *Continental Shelf Research*, 302, 105744.

Chilton D, Hamilton DP, Nagelkerken I, Cook P, Hipsey MR, Reid R, Sheaves M, Waltham NJ, and Brookes J (2021). Environmental flow requirements of estuaries: providing resilience to current and future climate and direct anthropogenic changes. *Frontiers in Environmental Science*. 9, 764218.

Chuang P, Young MB, Dale AW, Miller LG, Herrera-Silveira JA, and Paytan A (2017). Methane fluxes from tropical coastal lagoons surrounded by mangroves, Yucatán, Mexico. *Journal of Geophysical Research: Biogeosciences*, 122, 1156–1174.

DelSontro T, Boutet L, St-Pierre A, del Giorgio PA, Prairie YT (2016). Methane ebullition and diffusion from northern ponds and lakes regulated by the interaction between temperature and system productivity. *Limnology and Oceanography*, 61, S62–S77.

de Groot TR, Engelmann JC, Ramond P, Dorigo J, van Bleijswijk J, and Niemann H (2025). Adaptation of methane-oxidizing bacteria to environmental changes: implications for coastal methane dynamics. *Biogeosciences*, 22(19), 5173–5191.

Dunlop M, Grigg N, Ahmad M, and Rees G (2022). *Preliminary adaptation pathways for the Coorong, Lower Lakes and Murray Mouth*. CSIRO, Canberra.

IPCC (2021). *Climate Change 2021 – The Physical Science Basis: Working Group I Contribution to the Sixth Assessment Report of the Intergovernmental Panel on Climate Change*. Cambridge University Press, London.

Keneally C, Gaget V, Kidd SP, and Brookes JD (2024a). Sample preservation solution increases nucleic acid yield and environmental RNA quality in sediments across an estuarine salinity gradient. *Environmental DNA*, 6, e70016.

Keneally C, Southgate M, Chilton D, Gaget V, Welsh DT, Mosley L, Erler DV, Kidd SP, and Brookes JD (2024b). Organic matter accumulation drives methylotrophic methanogenesis and microbial ecology in a hypersaline coastal lagoon. *Limnology and Oceanography*, 69, 1970–1983.

Keneally C, Chilton D, Dornan TN, Kidd SP, Gaget V, Toomes A, Lassaline C, Petrovski R, Wood L, Brookes JD (2025a). Multi-omics reveal microbial succession and metabolomic adaptations to flood in a hypersaline coastal lagoon. *Water Research*, 280, 123511.

Keneally C, Gaget V, Chilton D, Kidd SP, Mosley L, Welsh DT, Zhou Y, Zhou L, and Brookes JD (2025b). Microbial ecology in hypersaline coastal lagoons: A model for climate-induced coastal salinisation and eutrophication. *Earth-Science Reviews*, 266, 105150.

Keneally C, Gaget V, Chilton D, Dornan TN, Hensel J, Keneally AE, Kidd SP, and Brookes JD (2026). Extreme salinity change governs microbial community assembly and interactions. *Environmental Microbiology Reports*, 18, e70301.

Li Y, Zhan L, Chen L, Zhang J, Wu M, and Liu J (2021). Spatial and temporal patterns of methane and its influencing factors in the Jiulong River estuary, southeastern China. *Marine Chemistry*, 228, 103909.

Li Y, Zhou Y, Zhou L, Zhang Y, Xu H, Jang K-S, Kothawala DN, Spencer RGM, Jeppesen E, Brookes JD, Davidson TA, and Wu F (2022). Changes in water chemistry associated with rainstorm events increase carbon emissions from the inflowing river mouth of a major drinking water reservoir. *Environmental Science & Technology*, 56, 16494–16505.

Maglaya RC, Sadat-Noori M, Andersen MS (2025). Groundwater discharge: A major driver of global methane emissions from aquatic environments. *Earth Systems and Environment*, 10, 2693–2705.

McMurdie PJ, and Holmes S (2013). phyloseq: an R package for reproducible interactive analysis and graphics of microbiome census data. *PLOS One*, 8, e61217.

Mosley L, Farkas J, Shao Y, and Fitzpatrick R (2022). *Monosulfidic Black Ooze (MBO) formation, cycling and management in the Coorong*. University of Adelaide, Adelaide.

Mosley L, Priestley S, Brookes J, Dittmann S, Farkaš J, Farrell M, Ferguson A, Gibbs M, Hipsey M, and Huang J (2023). Extreme eutrophication and salinisation in the Coorong estuarine-lagoon ecosystem of Australia's largest river basin (Murray-Darling). *Marine Pollution Bulletin,* 188, 114648.

Pfeiffer-Herbert AS, Prahl FG, Peterson TD, and Wolhowe M (2019). Methane dynamics associated with tidal processes in the Lower Columbia River. *Estuaries and Coasts*, 42, 1249–1264.

Poffenbarger H, Needelman BA, and Megonigal JP (2011). Salinity influence on methane emissions from tidal marshes. *Wetlands*, 31, 831–842.

Priestley S, Mosley L, Farkas J, Tyler J, Shao Y, Shanafield M, Banks E, Wong W, Leyden E (2022). *Sources and transport of nutrients in the Coorong*. Goyder Institute for Water Research Technical Report Series.

R Core Team (2021). R: A language and environment for statistical computing.

Rees G, Dunlop M, Grigg N, and Ahmad M (2022). T*rajectories of ecological change for the Coorong and Lower Lakes, in response to climate change*. CSIRO, Canberra.

Sadat-Noori M, Andersen MS, Rutlidge H, and Glamore W (2025). Coastal wetland restoration effects on carbon dynamics: a groundwater perspective. *Reviews of Geophysics*, 63, e2025RG000895.

Sø JS, Martinsen KT, Kragh T, Sand-Jensen K (2025). Ebullition dominates high methane emissions globally across all lake sizes. *Biogeochemistry*, 168, 43.

Sø JS, Sand-Jensen K, and Kragh T (2024). Self-made equipment for automatic methane diffusion and ebullition measurements from aquatic environments. *Journal of Geophysical Research: Biogeosciences*, 129, e2024JG008035.

Soued C, Bogard MJ, Finlay K, Bortolotti LE, Leavitt PR, Badiou P, Knox SH, Jensen, S., Mueller P, Lee SC, Ng D, Wissel B, Chan CN, Page B, and Kowal, P (2024). *Salinity causes widespread restriction of methane emissions from small inland waters*. *Nature Communications*, 15, 717.

Trifunovic B, Vázquez-Lule A, Capooci M, Seyfferth AL, Moffat C, and Vargas R (2020). Carbon dioxide and methane emissions from a temperate salt marsh tidal creek. *Journal of Geophysical Research: Biogeosciences*, 125, e2019JG005558.

Tweedley JR, Dittmann SR, Whitfield AK, Withers K, Hoeksema SD, and Potter IC (2019). *Hypersalinity: global distribution, causes, and present and future effects on the biota of estuaries and lagoons*, in: Coasts and Estuaries. Elsevier, pp. 523–546.

Villalobos Y, Canadell JG, Keller ED, Briggs PR, Ford, P, Harman IN, Hilton TW, Hogikyan A, Lauerwald R, Maher DT, Martinez A, Pan N, Poulter B, Resplandy L, Rosentreter JA, Saunois M, Tian H, Yeo J, and Zhang Z (2025). Methane and nitrous oxide budgets for Australasia: a regional assessment of natural and Anthropogenic Sources and Sinks. *Global Biogeochemical Cycles*, 39, e2024GB008484.

Welsh DT (2000). Ecological significance of compatible solute accumulation by micro-organisms: from single cells to global climate. *FEMS Microbiology Reviews,* 24, 263–290.

Wright MN, and Ziegler A (2017). ranger: A fast implementation of random forests for high dimensional data in C++ and R. *Journal of Statistical Software*, 77, 1–17.

Zhou Y, Zhang T, Zhou L, Zhang Y, Xu H, Jang, K-S, Drake TW, Grasset C, Davidson TA, Keneally CC, Brookes JD, and Jeppesen E (2025). Terrestrial organic matter inputs modulate methane emissions from a mega-reservoir. *Environmental Science & Technology*. 59, 6590–6599.


RESEARCH CENTRE
GOYDER
INSTITUTE
FOR WATER RESEARCH